PROGRESS IN COLOR, COLORANTS AND COATINGS

available online @ www.pccc.icrc.ac.ir

Progress in Color Colorants Coating 16 (2023), 31-45

Synthesis, Characterization and Corrosion Resistance Behavior of Waterborne Cationic Acrylic Resins

M. Haghi[1], Z. Ranjbar[1, 2*], H. Kazemian[3], M. Aghili[4]

[1.] Department of Surface Coatings and Corrosion, Institute for Color Science and Technology, P.O. Box: 16765-654, Tehran, Iran

[2.] Center of Excellence for Color Science and Technology, Tehran, Iran

[3.] Northern Analytical Lab Services (NALS), University of Northern British Columbia (UNBC), P.O. Box: 1000-9820, Prince George, BC, Canada

[4.] School of Chemical Engineering, College of Engineering, Queen's Universtity, P.O. Box: 438, Kingston, Ontario, Canada.

ARTICLE INFO

Article history:
Received: 27 Sept 2021
Final Revised: 18 Feb 2022
Accepted: 05 March 2022
Available online: 20 sep 2022

Keywords:
Acrylic resin
Cathodic electrocoating
Corrosion
EIS
Throwing power

ABSTRACT

Cationic acrylic resins with different glass transition temperatures (T_g) and molecular weight (M_w) were synthesized using different ratios of methyl methacrylate (MMA) and tertiary butyl acrylate (TBA) monomers. Furthermore, waterborne acrylic coatings were prepared using the cathodic electrocoating application technique. The cathodic electrocoating process was carried out at 80 V for 120 seconds to obtain a dry film thickness of 20±2 μm. Fourier transform infrared spectroscopy (FTIR), GPC (molecular weight), glass transition temperature, particle size, zeta potential, and viscosity measurements were used to characterize the synthesized cationic acrylic resin. The throwing power (ability to coat recessed area) and cross-cut adhesion were evaluated for each resin. According to the electrochemical impedance spectroscopy (EIS) data and general properties, the coatings with an MMA/TBA ratio of 0.125 exhibited excellent corrosion resistance (Log $|Z|_{0.01Hz}$ stay above seven even after 720 hours dipping in 3.5 wt.% NaCl solution). By increasing the MMA/TBA ratio, the final product's average molecular weight and viscosity were increased. Prog. Color Colorants Coat. 16 (2023), 31-45© Institute for Color Science and Technology.

1. Introduction

Waterborne acrylic base coating as a single-coat has been applied in a wide range of applications due to their interesting properties such as high resistance to weather and different solvents as well as their excellent appearance [1]. Acrylic resin is also considered a universal resin used in other coating processes due to its unique performance and variety of monomers. The cathodic electrocoating technique has been used in various industries as a unique coating application method [2]. Cathodic electrocoating can overcome some of the problems of the anodic electrodeposition coating technique, such as substrate dissolution and film discoloration, which may result in coatings with insufficient corrosion-resistance properties [3, 4]. Moreover, this method provides an excellent opportunity to produce a single-layer coating with sufficient weather and corrosion resistance under a mass-production scale, especially on objects with a complex shape, where the other painting application methods are rather tricky [5].

*Corresponding author: * ranjbar@icrc.ac.ir
Doi: 10.30509/PCCC.2022.166897.1135

Cathodic electrocoating is a powerful technique for film deposition on conductive substrates. In this process, direct current (D.C.) is applied for moving charged particles towards the electrode (i.e., conductive substrates) with the opposite charge to create a coating on the substrate. This application method has received much attention in the coating industry due to its excellent properties such as good corrosion resistance, uniform film, and superior throwing power, which is a measure of a cathodic electrocoating ability to form a uniform thickness even on recessed and un-accessible areas of complex shaped objects (cathodes) [6]. Furthermore, cationic acrylic coatings create a film with sufficient corrosion resistance [7]. Organic-based coatings act as a protective layer between the metal and corrosive agents as barrier coatings [8-13].

Suzuki has discussed film formation behavior of low and high Tg acrylic electrocoats, mainly focusing on the initiation process. Also, he has reported the influence of the Tg of resins on deposition behavior, using two cationic resins with different Tg values as model resins. He found that the film resistivity depends on Tg. There were two types of film formation, high resistance film formation behavior and ion-permeable film formation mechanism [14]. Usmani has reviewed anodic and cathodic electrodeposition. He has investigated the mechanisms, resins, and coating formulations and a brief discussion on electrochemical reactions [15]. Epoxy-acrylic microgels additives based on quaternary ammonium group were synthesized by dispersion polymerization. The effect of microgels on thermal flow was investigated. The results showed that the corrosion resistance has improved in presence of 7 % microgel additives [16].

There is enough research room to improve the throwing power and corrosion resistance properties of acrylic electrocoats. In this research work, three cationic acrylic resins, which contain an amino group in the backbone as a cationic group, were synthesized with different molecular weights using various monomers. The cationic resin is neutralized by lactic acid and dispersed in water. Products with different molecular weights were obtained using different monomers' ratios. Detailed analysis of the performance of the developed coatings is presented and discussed based on throwing power and general coatings properties. The anticorrosion performance of prepared coatings is presented and discussed based on electrochemical impedance spectroscopy (EIS) data. The main objective of current research is an investigation of the effect of the molecular weight of the synthesized cationic acrylic resin on the cathodic electrocoating behavior and corrosion resistance of synthesized coatings.

In this study, for the first time, the particle size mitigation ability and stability of high molecular weight acrylic cationic dispersion resin and also the impact of the particle size on throwing power, adhesion, and zeta potential were studied.

2. Experimental

2.1. Materials

Tert-butyl acrylate (TBA), 2-ethyl hexyl acrylate (2EHA), methyl methacrylate (MMA), dimethyl aminoethyl methacrylate (DMAEMA), 2,2 bis azo isobutyl nitrite (AIBN), butyl glycol(B.G.), isopropyl alcohol (IPA), and lactic acid were purchased from Sigma-Aldrich (Germany). Alkylated melamine formaldehyde as a crosslinking agent was supplied by Allnex (The Netherlands). Throughout the project, deionized water (conductivity: 15±5 $\mu S.cm^{-1}$, pH: 6.5) was used. All the materials were reagent grade and used as received without further purification. The physical properties of the used monomers are summarized in Table 1.

Table 1: Physical properties of the monomers.

monomer	Tg (°C)	Mw (g/mol)	Viscosity @ 20 °C (cP)
HEMA	76.85	130.14	6.1
2EHA	-52.15	184.27	1.7
MMA	105	100.121	0.6
DMAEMA	18.85	157.21	1.34
TBA	37.85	128.17	0.9

2.2. Synthesis of cationic acrylic resins

The polymerization reaction was carried out in a 500 mL four-necked round-bottom glass flask. The flask was equipped with a mechanical stirrer, water-cooled reflux condenser, a thermometer, and a feed dropping funnel. A silicon oil bath was used as the heating source. In a typical experiment, the solvents consisting of isopropyl alcohol and butyl glycol were introduced into the reactor vessel and were mixed while heated at 80 °C under reflux (atmospheric pressure). Different ratios of MMA/TBA of 9, 1, and 0.125 were used to prepare cationic resins with different Tg and Mw (Table 2). In order to synthesize acrylic resins, the monomers and the initiator are mixed in a separate vessel with a mechanical stirrer for 30 minutes to dissolve the initiator powder in the monomers completely. Then the proper mixture of monomers (MMA, TBA, HEMA, EHA), initiator (AIBN), and a functionalized amine monomer (DMAEMA) were added into the reactor through dropping funnels in three hours.

Finally, the reaction mixture was held at 90 °C for an additional 3 hours to continue the polymerization reactions. Throughout the text, AC (X) stands for acrylic resin containing the "X" ratio of methyl methacrylate to tert-Butyl acrylate. The endpoint of each reaction was determined via nonvolatile content measurements (ASTM D7232- 06(2016)). The reaction was terminated at a solid content of 67±1% for each synthesized resin. Furthermore, dimethyl amino ethyl methacrylate (DMAEMA) was used as a cationic component due to nitrogen functional groups in its structure. The schematic polymerization reaction is shown in Figure 1.

2.3. Substrate preparation

The aluminum sheet substrates (7.5 × 15 × 0.7 cm) kiyapanel AL 0.7 were supplied from Kiyafarin Co (Iran) and stainless steel 316 with the same size were used as a cathode and anode, respectively. Before cathodic electrocoating, the substrates were degreased with acetone, rinsed with deionized water, and dried at room temperature.

2.4. Neutralization of cationic acrylic resins

In order to make a dispersion of the synthesized resins in the water, the acrylic resins with different Mw and Tg were neutralized using lactic acid (80 wt. %) and diluted with deionized water. So, 430 g of the waterborne acrylic resin was added into a reactor vessel (equipped with a mechanical stirrer) followed by adding 75.25 g of alkylated melamine-formaldehyde as a crosslinking agent at 1000 rpm for 60 min. At this stage, 26.5 mL of lactic acid (80 wt. %) was added to neutralize the nitrogen groups for making a cationic resin dispersions suitable for the cathodic electrocoating process. Then, 140 mL deionized water was added slowly in three steps. The mixture was stirred at 160 rpm for 120 min until a stable dispersed resin in water was formed. To eliminate the effect of resin concentration in the properties, the nonvolatile content of the cathodic electrocoating baths was kept constant at 10±1 for all resin dispersions.

Table 2: The composition of different cationic acrylic resins.

Sample	AC (09)	AC (01)	AC (0.125)
HEMA[a]	20	20	20
2EHA[b]	10	10	10
MMA[c]	45	25	5
DMAEMA[d]	20	20	20
TBA[e]	5	25	45
B.G.	40	40	40
IPA	10	10	10
AIBN	2	2	2
SUM	152	152	152
MMA/TBA	9	1	0.125

[a.] HEMA=(Hydroxyethyl) methacrylate; [b.] 2EHA= 2-Ethylhexyl acrylate; [c.]MMA= Methyl methacrylate
[d.] DMAEMA= di methyl amino ethyl methacrylate; [e.] TBA= tert-Butyl acrylate

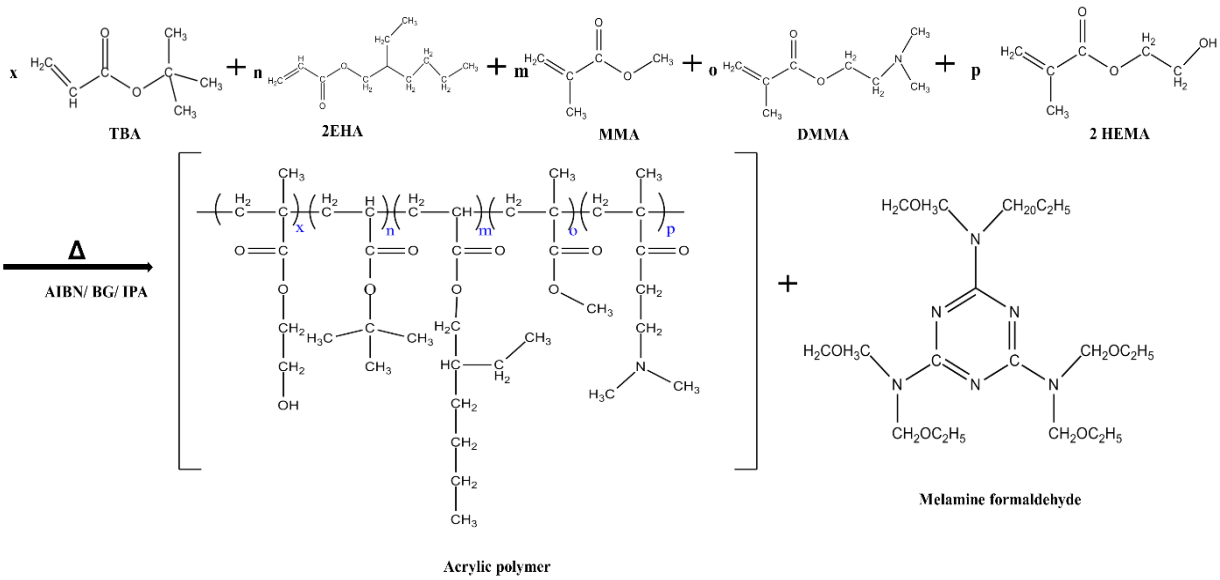

Figure 1: The schematic chemical reaction of monomers.

The ingredients of the different waterborne acrylic dispersion are summarized in Table 3. The neutralization of acrylic resins is illustrated in Figure 2. Characteristics of the cathodic electrocoating bath including the synthesized resins of AC(09), AC(01), and AC(0.125) are shown in Table 4. In this Table the MEQ is the number of milliequivalents of lactic acid per 100 g of nonvolatile contentof resin (ASTM D7232 -06(2016) that was measured by potentiometric titration (PSA PEUGEOT-CITROEN D551017). The characteristics of synthesized resin are summarized in Table 5.

The CED process was conducted at a constant D.C. voltage of 80V with a constant time span of 120 sec. The aluminum substrate was used as the cathode, and a 304 stainless steel plate was used as the anode. In order to obtain a thickness of 20±2 µm of dry film, a constant concentration of 10 wt. % of each resin in water was used. The two electrodes were lined up vertically with a distance of 10 cm. Magnetic stirring was employed to maintain the homogeneity of the dispersed particles throughout the cathodic electrocoating process.

Table 3: Components for neutralization of acrylic resins.

Compound	amount (g)
Water	140.00
Lactic acid	26.488
AC(09), AC(01), AC(0.125)	430.00
Alkylated melamine formaldehyde crosslinking agent	75.25

Table 4: Characteristics of the cathodic electrocoating bath for each type of synthesized resin.

Characteristic	AC(09)	AC(01)	AC(0.125)
Bath solid content 105 °C @3 hrs.	10±1	10±1	10±1
Bath pH	6.09±0.1	5.95±0.1	5.8±0.1
Bath conductivity	1720±20 $\mu S.cm^{-1}$	1662±20 $\mu S.cm^{-1}$	1732±20 $\mu S.cm^{-1}$
Bath MEQ*	75±3	75±3	75±3
MEQ*= milliequivalent of lactic acid per 100 g of nonvolatile content of resin			

Table 5: Characteristics of synthesized resin (AC (09), AC (01), and AC (0.125)).

Characteristic	AC(09)	AC(01)	AC(0.125)
Resin hydroxyl value	86 ±1 mmol/g-solid	86 ±1 mmol/g-solid	86 ±1 mmol/g-solid
Resin viscosity at 23 °C	238±2 Pa.s	187±2 Pa.s	4.8±2 Pa.s
Resin solid content 105 °C @3 hrs	67±1	67±1	67±1

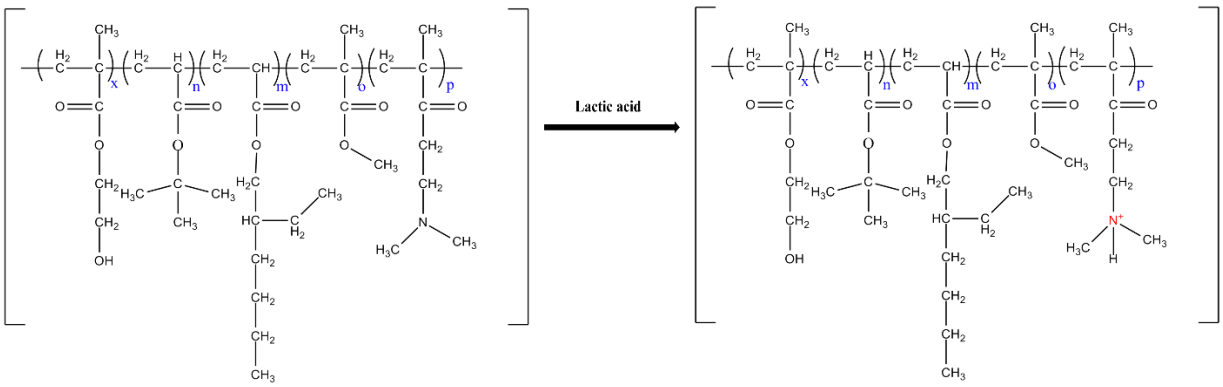

Figure 2: The neutralization of acrylic resin for the cathodic electrocoating process.

When the cathodic electrocoating was completed, the coatings were rinsed with deionized water and then cured in an oven at 170±2 °C for 20 min.

2.5. Characterization methods

Fourier transform infrared spectroscopy (FTIR) (Model Spectrum 3 from Perkin Elmer, USA) was used to structural analysis of the synthesized acrylic resins. Gel permeation chromatography (GPC) (Waters 1515-2414, China) was used to determine molecular weights and distributions (Narrow molar mass poly(methyl methacrylate) (PMMA) standards were used for the universal calibration. The synthesized resin's particle size was measured using a Better size 2000 particle size analyzer (China).

The glass transition temperature (Tg) of acrylic resins was determined using a differential scanning calorimetry (DSC) Nanjing Dazhan Institute of Electromechanical Technology, China). For a typical DSC analysis, the temperature was increased from -50 to 100 °C at a heating rate of 10 °C/min under a nitrogen atmosphere. The Tg was determined as the onset of the change of slope of the measurement curve. The zeta potential values were measured using a Zetameter (Zen 3600, Malvern) by adjusting the pH at 5.9 at 25 °C.

The viscosity was measured by a DV-3 ULTRA viscometer (Brookfield, USA) at 23 °C. During all the experiments, pH and conductivity were measured using a pH/conductivitymeter, (914 METROHM, Switzerland). The current density-time during the cathodic electrocoating process was recorded by a multi-meter (model ms-1600, nikkiso Group, Japan).

2.5.1. Throwing power

One of the most essential cathodic electrocoating process features is the inherent throwing power of the coating material. The throwing power of the acrylic dispersion was measured by a tube penetration test, which includes an aluminum strip sheet (ASS) connected to the cathode and a stainless steel (ST 304) tube connected to the anode [16, 17]. The ASS strip is immersed into the ST 304 tube containing the acrylic dispersion. The ASS is rinsed with deionized water and cured in an oven at 170±2 °C for 20 min. The height of coated ASS (in cm) with acrylic dispersion is defined as the throwing power. In this study, a constant DC voltage of 80 V was applied for 2 min. to measure the throwing power.

2.5.2. Cross-cut adhesion test

The adhesion strength of the developed coatings was evaluated by the cross-cut test according to the ASTM D3359-17 guidelines, using a cross-cut tester (Elcometer 104, U.K.). The cut distance was 1 mm, drawing the handle with the appropriate cutter through the coating

into the substrate and making the lattice pattern. An adhesion test result is classified between 0-5.

2.5.3. Corrosion evaluation procedure

Corrosion protection attributes of the developed coatings were evaluated by electrochemical impedance spectroscopy (EIS). The EIS was performed in a three-electrode cell, including Ag/AgCl, platinum wires, and coated steel strips as the reference electrode, counter electrode, and working electrode. The test was conducted on 1 cm^2 of the steel samples coated with synthesized acrylic resin immersed in 3.5 wt. % NaCl electrolyte solution using a Potentiostat (Ivium Compactstat, Netherlands) at different immersion times ranging from 30 min to 30 days. The obtained EIS data were interpreted using the ZSimpWin software.

3. Results and Discussion

3.1. Chemical structure of the acrylic resin

The FTIR spectra of the cationic acrylic resins are presented in Figure 3. The characteristic absorption band at 3428 cm^{-1} can be attributed to the O-H (stretching) functional group of the synthesized resins. Absorption peaks at 2953 and 2876 cm^{-1} can be attributed to the C-H (stretching) for CH_3 and CH_2 of the acrylate polymer, respectively. Moreover, the peaks at 1733, 1458 and 1246 cm^{-1} have corresponded to the C=O, –COO–, and C-N stretching of the acrylate polymer, respectively. Because the amine group is tertiary amines (R3N), it does not show any sharp band in the 3300-3000 cm^{-1} region. Absorption peaks at 1387 (CH_3 vibration) and 1157 cm^{-1} (O=C–O–C– vibrations) could be ascribed to the formed acrylate polymers. The FTIR absorption peak that appeared at 845 cm^{-1} could be attributed to the stretching vibration of C=O of the acrylate group. The peak at 744 cm^{-1} is a characteristic absorption peak of C–H (stretching) in TBA. On the other hand, the C=C absorption peak of the monomers in the range of 1500 and 1700 cm^{-1} were disappeared at the FTIR spectrum. From the FTIR data, it can be concluded that the cationic acrylic polymer resin was synthesized successfully. It means all of the monomers are participated (consumed) in the copolymerization reaction.

3.2. Glass transition temperature

The glass transition temperature (Tg) of each resin was determined using DSC techniques. As it can be seen from the results shown in Table 6, AC(09) showed the highest Tg, while AC(0.125) exhibited the lowest Tg (Table 6). This trend can be attributed to the ratio of MMA/TBA of each sample. The Tg of MMA is 105 ^oC which is much higher than the Tg of TBA, 37.85 ^oC.

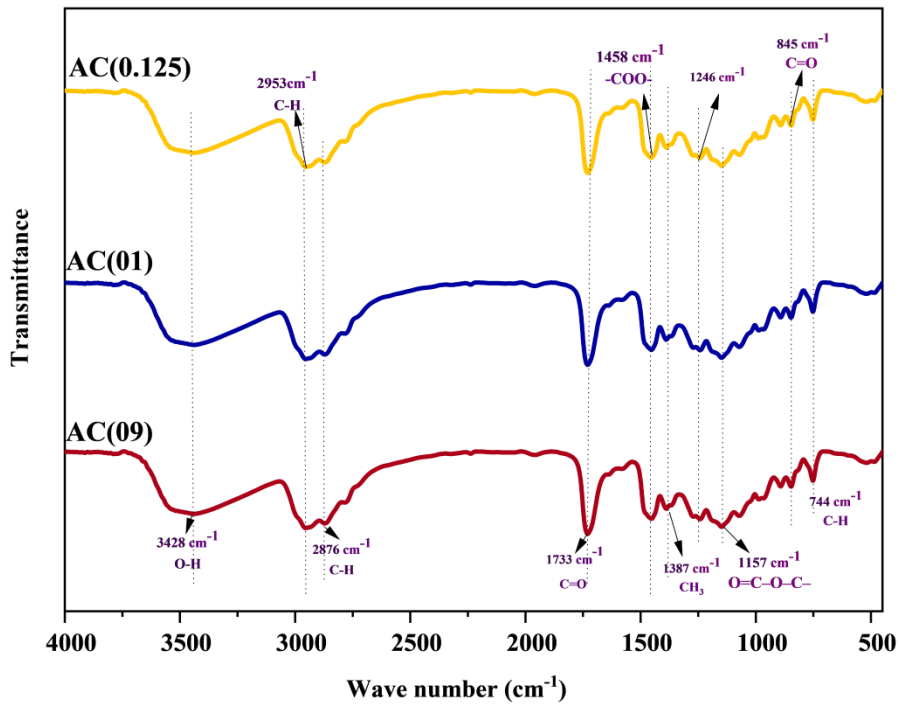

Figure 3: FTIR spectra for cationic acrylic resins.

Table 6: The value of Tg for synthesized resins.

Resin type	Tg (^{o}C)
AC (09)	46.1±1
AC (01)	35.1±1
AC (0.125)	18±1

Table 7: The molecular weight of synthesized acrylic resins by GPC

Resin type	Mn (g/mol)	Mw (g/mol)	Mw/Mn
AC(09)	58953	84557	1.4
AC(01)	12630	20580	1.6
AC(0.125)	7283	12371	1.7

Mn: number average molecular weight;
Mw: weight average molecular weight
Mw/Mn: polydispersity index

3.3. GPC analysis

Table 7 shows the synthesized resin's average molecular weights (Mn and Mw) and polydispersity index (Mw/Mn).

AC(09) sample exhibited the highest and AC(0.125) showed the lowest molecular weights. Materials of higher molecular weights exhibit a greater degree of molecular attraction and entanglement, greater rigidity and strength, and higher glass transition temperature. The AC(09) sample in this study showed the highest glass transition temperature (Table 6).

The polydispersity index (Mw/Mn), which is a measure of the molecular weight distribution [19] of AC(09), AC(01), and AC(0.125) samples were 1.4, 1.6, and 1.7, respectively. By decreasing the MMA/TBA ratio from 9 to 0.125, the molecular weight shifted toward lower numbers, while the distribution range remained more or less the same.

3.4. Viscosity

The measured viscosities of the synthesized resins are summarized in Table 8. As it could be seen, the higher the molecular weights, the higher viscosities. The viscosity of a dispersed resin mixture in water could be controlled by changing the bath's resin concentration.

3.5. Particle-size of the waterborne acrylic resin dispersions

The particle size distributions of the synthesized cationic acrylic resin dispersions are shown in Figure 4 and Table 9. The appearance of AC(09), AC(01), and AC(0.125) samples were milky/opaque.

A relatively unimodal distribution for AC(01) and AC(0.125) and AC(09), with particle sizes of 60 to 1400 nm, was observed. It was found that the AC(09) resin with a higher molecular weight exhibited a smaller particle size range and narrower size distribution. The AC(0.125) resin sample with the lower molecular weight showed overall larger particles and broader size distribution.

Table 8: The synthesized resin viscosities.

Resin type	Viscosity (cP) (at 23°C)
AC(09)	237000
AC(01)	18700
AC(0.125)	4860

Table 9: Particle size analysis of resin dispersions.

Sample	D10	D50	D90
AC(09)	0.104	0.225	0.531
AC(01)	0.132	0.368	1.163
AC(0.125)	0.483	0.678	1.293

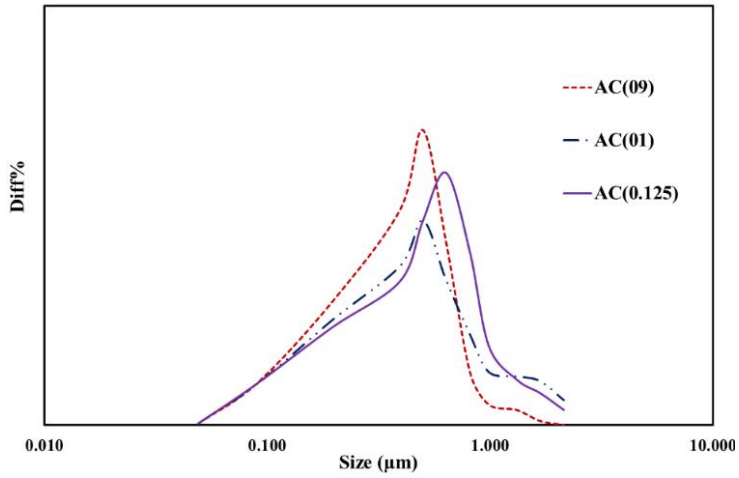

Figure 4: The particle size distribution of the resins (AC(09), AC(01), and AC(0.125)).

Since the particle size is directly related to the degree of neutralization, the higher degree of neutralization, the lower particle size in dispersion [26]. A stoichiometric amount of lactic acid (26.488 g) was used to neutralize the resin (430 g).

3.6. Zeta potential of waterborne acrylic dispersions

According to the zeta potential results (measured at pH= 5.9), the resins' surface charge is positive (Figure 5). Positively charged resins are suitable for the cathodic EPD process because of their tendency toward the cathode. For all samples, the zeta potential value was higher than 30 mV (at pH= 5.9), which means the EPD baths were stable during the process because the electrostatic repulsion force is likely strong. As a result, at this pH all resins are stabilized based on the fact that the zeta potential greater than a reference value of 30 mV could give a strong electrostatic repulsion forces among resins' particle.

In high molecular weight, cationic acrylic resin zeta potential is 92.6 mV, and for low molecular weight resin is 60 mV. These numbers show resin with higher molecular weight has better stability without sedimentation in electrocoating bath.

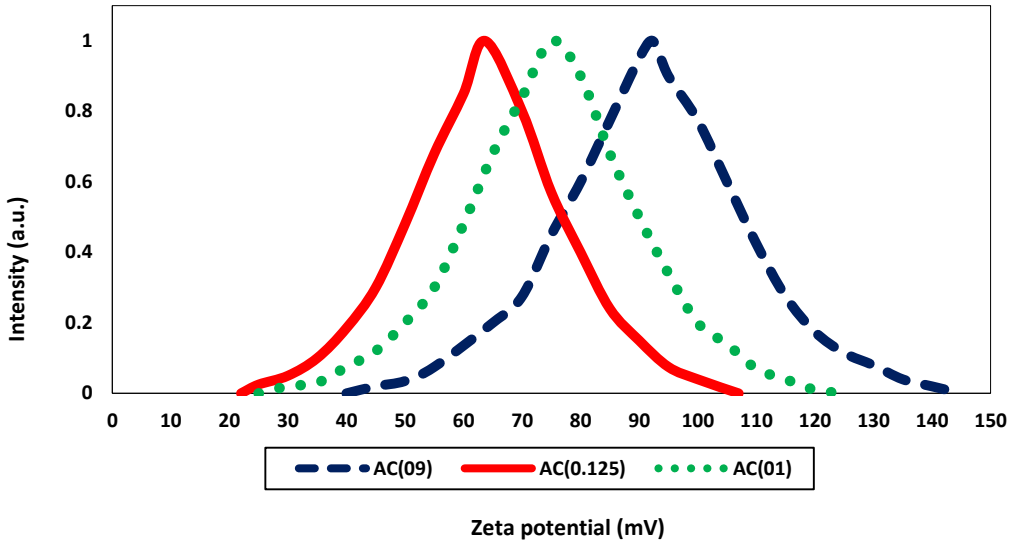

Figure 5: Zeta potential measurements of the synthesized resins.

3.7. Throwing Power

The throwing power of the resin dispersions is reported in Table 10. As it can be seen, the AC(09) sample exhibited the highest throwing power meaning this resin has the highest capability to make a uniform and resistive film on the surface. According to Furono [28], throwing power coming back to the resistivity of deposited film and conductivity of bath in these cases, the conductivity of baths are the same for all sample, so resistivity of the film is the main affecting factor on throwing power. This observation can be attributed to the higher electrocoagulated film resistivity and lower ion permeability of the resins with higher molecular weight and Tg [16].

3.8. Electrodeposited film characteristics

3.8.1. Current density diagrams

The cathodic electrocoating process was performed at 80 V for 120 seconds. Electric current was recorded and normalized on the electrode surface during the deposition process to yield current density. The current density was plotted versus time for waterborne acrylic dispersions (Figure 6). It was observed that the current density was decreased abruptly, which can be attributed to the formation of an insulating film on the electrode surface (i.e., the conductive metal electrodes become an insulated surface in the circuit) [26]. However, declining current density indicates the thickening of the coatings, which acts as an insulating layer on the electrode surface, inhibiting electrical current flow. At the voltage 80 V, the residual current density is lowest for high molecular weight resin AC(09). On the other hand, the film resistance depends on resin structure, and film resistivity of the high Tg resin is more elevated than low Tg resin [27]. Thus, resin's electrodeposition behavior with high molecular weight and Tg showed a lower current density as the film becomes more insulating.

Table 10: The throwing power of the waterborne acrylic dispersions.

Sample	Throwing power (cm)
AC(09)	15±0.5
AC(01)	13.5±1
AC(0.125)	10±0.5

The electrodeposited samples were then cured at 170 °C for 20 minutes. The thickness of all coatings was 20±2 µm.

3.8.2. EIS characterization

The anticorrosion performance of coatings was evaluated at various immersion times (30 min to 720 hrs) in a 3.5 wt. % NaCl solution using the EIS technique. The Bode plots, phase angle, and Nyquist diagrams are depicted in Figures 7, 8 and 9, respectively.

The ZSimpwin software was used to fit the EIS data, which are shown as solid lines. The capacitive loops at low frequencies, the Nyquist plots at low frequencies are magnified (Figure 8).

The impedance value at ten mHz (log|Z|0.01 Hz) is illustrated in Figure 9. As shown in Figure 9, Log |Z| 0.01 Hz for AC(09) after 72 hours dropped below 6, and after 720 hours, this value is at 4, which depicts that AC(09) lost its anticorrosion performance and failed. On the other hand, this value for AC(01) and AC(0.125) is above seven even after 720 hours, which means these samples exhibited better barrier performance. This result shows resin with lower molecular weight (AC(0.125) revealed better anticorrosion performance. This can be attributed to lower molecular weight can result in higher crosslinking density and better adhesion properties. The corrosion protection performance of these samples did not change significantly. The phase angle plots which support the observations are shown in Figure 7. Indeed, the phase angle for AC(09) is not 90° at high-frequency even after 30 minutes of immersion, whereas in the AC(01) and AC(0.125) stays at 90° up to 720 hours. Both AC (01) and AC(0.125) samples did not show any significant reduction in phase angle value. This value did not change much for AC(01) and AC(0.125) after 720 hours of immersion.

These results indicate better anticorrosion performances for AC(01) and AC(0.125) samples compare to AC(09). As it can be seen in Figure 8, an evident trailing semicircle corresponding to two-time constants appeared for AC(09) sample after 720 hours.

This phenomenon for AC(09) sample can be attributed to the fact that the coatings' protective characteristic may decline, and the corrosion reactions were initiated at the metal/coating interface. Technically speaking, as the time constants refer to barrier performance of organic coatings [20, 28], therefore, AC(01) and AC(0.125) samples did not show

any evident corrosion at the same time.

After 720 hours of immersion, the AC(0.125) sample showed the highest resistance among the tested samples. Indeed, this sample shows superior coating performance when using a higher amount of TBA monomer compared to others. Lower hydrolysis of the hydrogen bonding in the metal-coating interface and more inadequate corrosion reaction is due to the higher phase angle of these samples.

ZSimpwin software was used for curve fitting of EIS data, shown as the black lines in the diagrams. Moreover, this software was used to fit an equivalent circuit, as shown in Figure 10. The equivalent circuit (a) was used for all samples when the corrosive agents are not reached the metal-coating interface yet.

As soon as the corrosive agents are reached the interface, a double layer will be created. The equivalent circuit (b) was used to illustrate the situation. All these electrochemical parameters are summarized in Table 11.

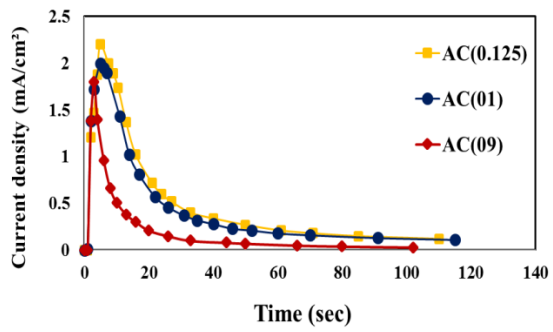

Figure 6: Current density versus time diagram for deposition of synthesized acrylic resins.

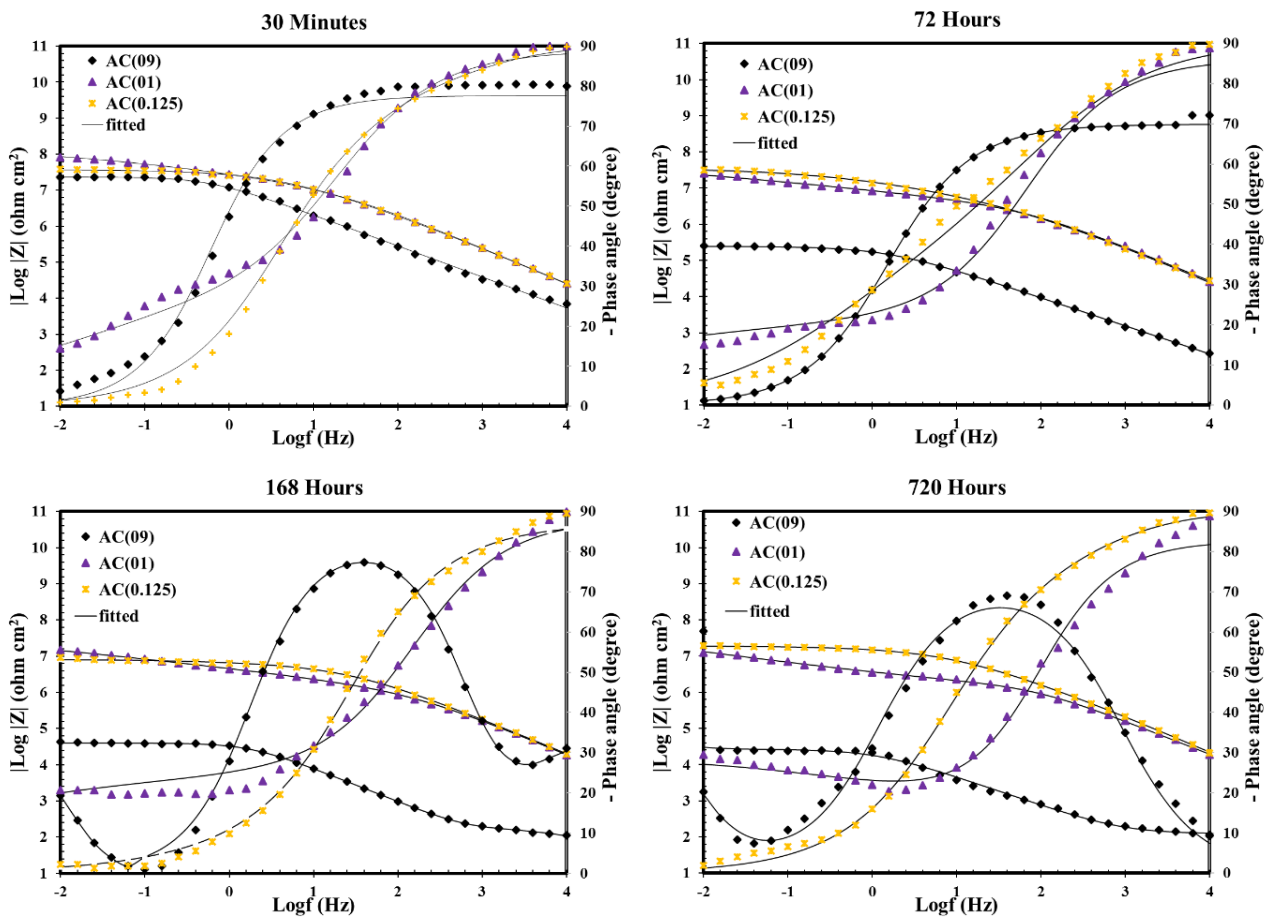

Figure 7: Bode plots of the samples during different immersion times in 3.5 wt. % NaCl solution.

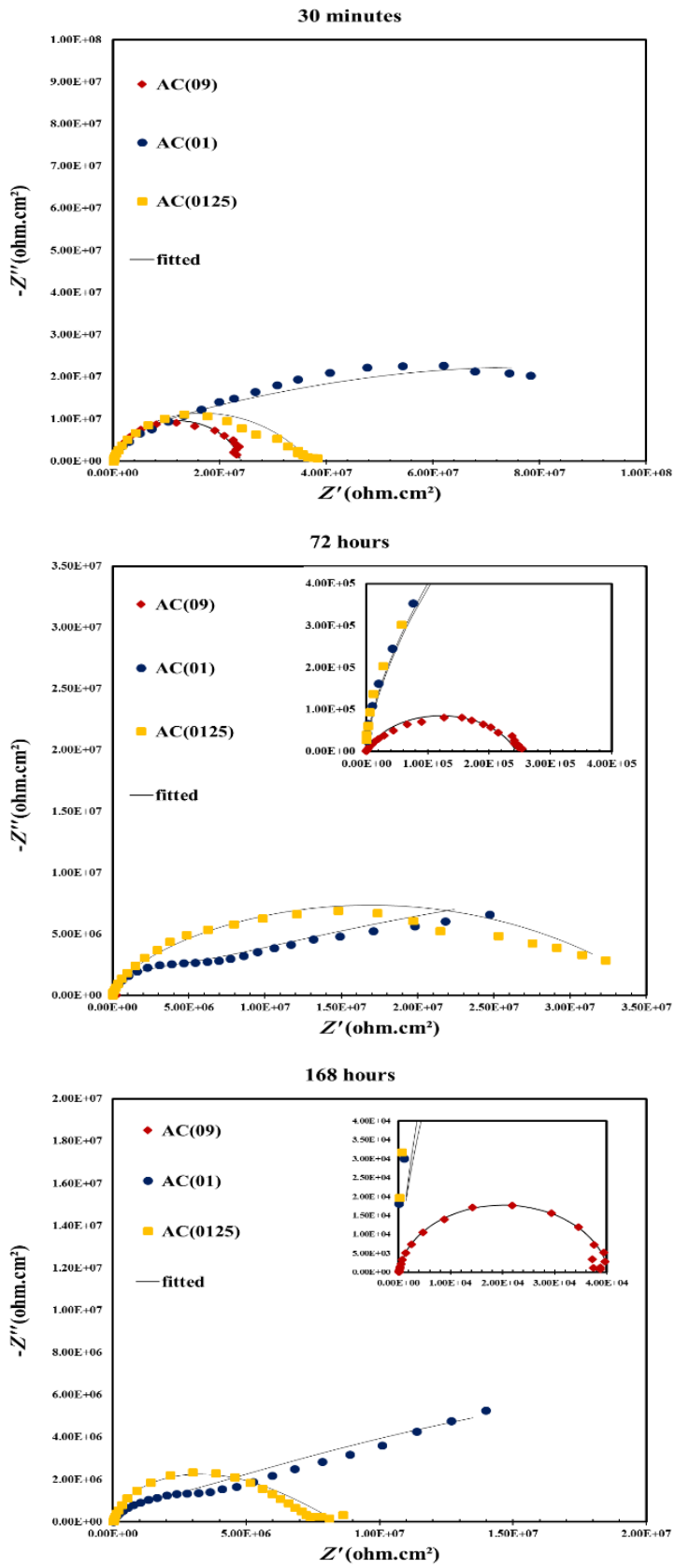

Figure 8: Nyquist plots of the samples during different immersion times in 3.5 wt. % NaCl solution.

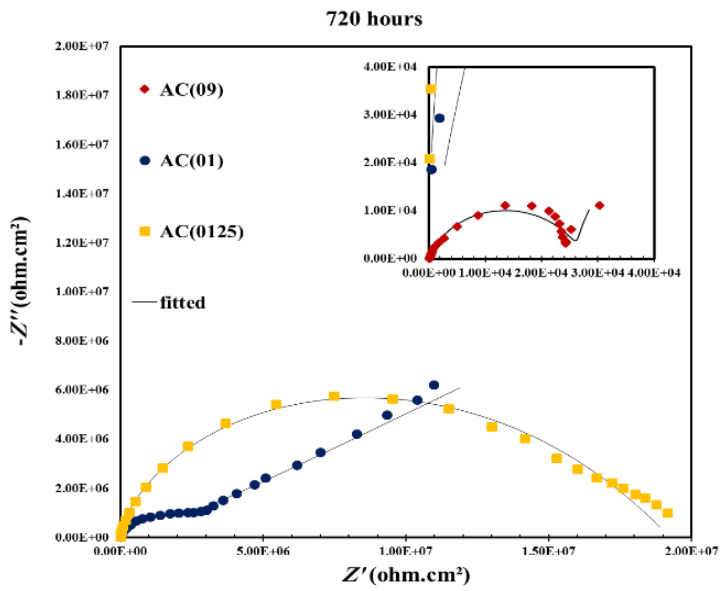

Figure 8: Continue.

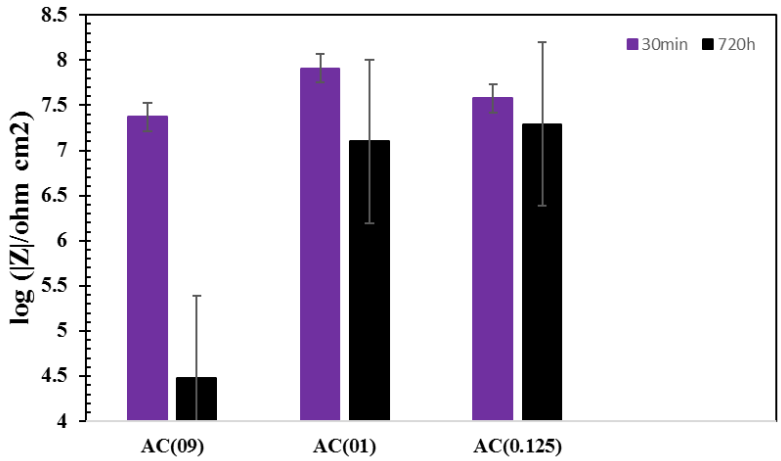

Figure 9: The impedance values at ten mHz of the samples after 30 minutes and 720 hours of immersion.

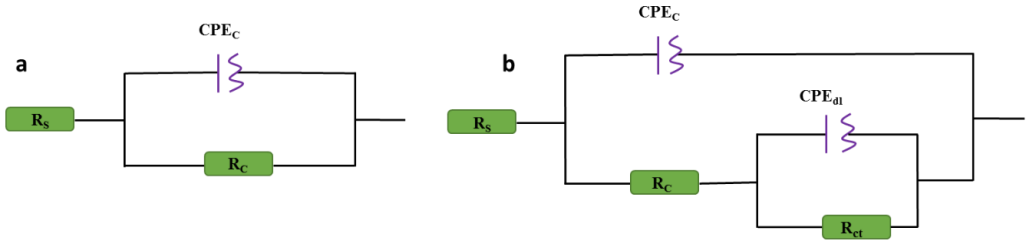

Figure 10: The equivalent circuit used to fit the EIS experimental data: (a) before, (b) after reaching corrosive agents to the metal-coating interface.

Table 11: The electrochemical parameters extracted from impedance data of the samples.

Sample	Time	R_c (Ω cm^2)	R_{ct} (Ω cm^2)	CPE_c		Cc ($F.cm^{-2}$)	CPE_{dl}		C_{dl} ($F.cm^{-2}$)	Chi-square
				Q ($\Omega^{-1}.cm^{-2}.s^{\alpha}$)	α		Q ($\Omega^{-1}.cm^{-2}.s^{\alpha}$)	α		
AC (09)	30 min	2.393E7	-	1.337E-8	0.8628	1.11E-09	-	-	-	1.340e-02
	72 hours	2.441E5	6.532E4	7.162E-8	0.7761	1.22E-09	1.32E-9	0.8293	1.14E-11	5.727e-03
	168 hours	4.534E4	5.125E4	1.014E-9	0.7248	1.26E-09	1.707E-9	0.8129	4.21E-10	9.231e-03
	720 hours	2.698E4	5.106E4	7.192E-9	0.7112	1.02E-09	1.57E-8	0.768	2.64E-10	1.627e-02
AC (01)	30 min	1.591E8	-	1.542E-8	0.9881	1.55E-08	-	-	-	3.818e-03
	72 hours	7.336E7	1.004E8	9.363E-10	0.9572	8.30E-08	6.622E-9	0.678	1.22E-14	6.859e-03
	168 hours	4.445E6	6.379E7	1.001E-9	0.9432	9.06E-08	1.207E-9	0.6235	4.82E-14	3.552e-03
	720 hours	1.097E6	4.563E7	2.006E-9	0.9118	1.16E-08	1.984E-8	0.6118	8.09E-13	4.877e-03
AC (0.125)	30 min	3.616E7	-	4.491E-9	1	4.44E-11	-	-	-	1.865e-03
	72 hours	6.993E6	1.858E7	7.127E-10	1	7.12E-11	7.364E-9	0.9499	1.99E-14	9.532e-04
	168 hours	3.887E6	8.408E6	1.688E-10	0.8169	7.46E-10	1.086E-9	0.9697	3.70E-13	2.834e-03
	720 hours	1.483E5	3.589E6	6.315E-10	1	5.31E-10	1.825E-8	0.9684	4.64E-13	5.868e-03

The effective capacitance values (Cdl) were evaluated by the Brug equation (Eq. 1) [21, 22]. The capacitance values (Cc) were estimated by the Hsu and Mansfeld formula (Eq. 2) [23, 24]. The data are shown in Table 10.

$$C_{dl} = Q^{1/\alpha}.\left(\frac{Rs\ Rct}{Rs+Rct}\right)^{(1-\alpha)/\alpha} \quad (1)$$

$$C_c = Q^{1/\alpha}.R_c{}^{(1-\alpha)/\alpha} \quad (2)$$

Where the α (0< α <1) and Q are known as exponent and admittance of the corresponding CPE element, respectively [25]. As the surface homogeneity enhances and the rime when the corrosive agents don't reach the surface, the value of α approaches one, representing an ideal capacitor. According to the Table 10, α value for most is not 1, which means that the coating is far from the ideal capacitor and corrosive agents penetrate the metal surface.

According to Table11, the value of Rct decrease by increasing the immersion times while the Cdl (calculated by Eq. 1) rises for all samples because of diffusing of electrolyte to the interface. Increasing the value of Cdl indicates that a porous rust film is formed on the coating. As shown in the Table 11, the coating capacitance (Cc) demonstrates the water permeability of the coating. Therefore, lower coating capacitance (Cc) for a coating indicates lower water absorption (lower corrosion agent) that eventually leads to more minor Corrosion. As it can be seen from Table 11, the Cc is lower for AC(01) and AC(0.125), which means these samples absorb less water according to the high value of water capacitance compared to the AC(9) coating. Indeed, AC(01) and AC(0.125) limited the diffusion of the electrolyte through the resin to the interface, which led to slower depression of the Rct values for these samples. Moreover, Cdl increases for these samples by immersion time indicates that a porous rust film is formed on the coating.

The coating resistance shows higher resistance during the first hour of immersion, particularly for the AC(01) and AC(0.125) samples, and remains almost constant for these samples during all exposure times while this value declines after 720 hours for AC(09), significantly. Therefore, it can be concluded that the AC(01) and AC(0.125) resins show excellent anticorrosion performance in comparison to the AC(09) resin.

3.9. Cross-cut adhesion test

The results of the cross-cut adhesion test are shown in

Table 12. All samples have an acceptable adhesion to be used for coating purposes. The AC (0.125) highest adhesion characteristic can be attributed to its functional groups leading to increased hydrogen bonding between the coating and surface.

Table 12: The cross-cut adhesion and gloss tests result performed on the samples.

Resin type	Adhesion
AC(09)	4B
AC(01)	4B
AC(0.125)	5B

4. Conclusion

The cathodic electrocoating process was successfully utilized to manufacture uniform cationic acrylic resin coatings (with controlled thickness) with different molecular weights and glass transition temperatures using different MMA/TBA ratios. The synthetic cathodic acrylic resins possessed positive charges, which made the resin particle migrate toward the cathode in a cathodic electrocoating bath.

The results show that the molecular weight and glass transition temperature of cationic acrylic electrodeposition resins play an essential role in properties such as particle size and throwing power, and adhesion and corrosion resistance. Increasing molecular weight and glass transition temperature improve throwing power and decreasing particle size. But they do not necessarily improve corrosion resistance. Therefore, adhesion is an essential factor in enhancing corrosion resistance.

5. References

1. M. Calovi, et al., Effect of functionalized graphene oxide concentration on the corrosion resistance properties provided by cataphoretic acrylic coatings, *Mater. Chem. Phys.*, 239(2020), 121984.
2. M. Bakhtiary-Noodeh, S. Moradian, Z. Ranjbar, Improvement of the edge protection of an automotive electrocoating in presence of a prepared epoxy-amine microgel, *Prog. Org. Coat.*, 103 (2017), 111-125.
3. S. Esfahani, Z. Ranjbar, S. Rastegar, Comparison of corrosion protection of normal and galvanised steel coated by cathodic electrocoatings using EIS and salt spray tests, *Corros. Eng. Sci. Techol.*, 51(2016), 82-89.
4. M. Bakhtiary-Noodeh, S. Moradian, Z. Ranjbar, Edge protection improvement of automotive electrocoatings in the presence of silica nanoparticles, *Surf. Coat. Technol.*, 317(2017), 134-147.
5. M. Rashvand, Z. Ranjbar, Cathodic electrodeposion of nano Titania along the epoxy based coating and evaluation of its anticorrosion properties, *Prog. Color, Colorants Coat.*, 7(2014), 227-235.
6. YI. Suzuki, Fukui H, Tsuchiya K, Ogata YH. Initiation process of film formation for cationic electropaint system, *J. Electrochem. Soc.*, 147(2000), 3700.
7. K. Ismoilov, et al., Synthesis and evaluation of properties of a novel cationic waterborne polyurethane finishing agent, *J. Chem. Eng. Process. Technol.*, 10(2019), 398.
8. A. A. Olajire, Recent advances on organic coating system technologies for corrosion protection of offshore metallic structures, *J. Mol. Liq.*, 269(2018), 572-606.
9. R. G. Hu, et al., Recent progress in corrosion protection of magnesium alloys by organic coatings, *Prog. Org. Coat.*, 73(2012), 129-141.
10. S. L. Esfahani, Z. Ranjbar, S. Rastegar, An electrochemical and mechanical approach to the corrosion resistance of cathodic electrocoatings under combined cyclic and D.C. polarization conditions, *Prog. Org. Coat.*, 77(2014), 1264-1270.
11. S. Morsch, S. Lyon, S. Gibbon, The degradation mechanism of an epoxy-phenolic can coating, *Prog. Org. Coat.*, 102(2017), 37-43.
12. V. S. Sastri, Corrosion inhibitors: principles and applications, Wiley pub., New York, 1998.
13. V. Ashworth, C. Booker, Cathodic protection: Theory and practice, Wiley pub., New York, 1986.
14. H. S. Jazi, Advanced plasma spray applications, BoD–Books on Demand pub., 2012.
15. Z. Ranjbar, et al., Effects of nano silica on the Anticorrosive properties of epoxy coatings, *Prog. Color Colorants Coat.*, 6(2013), 119-128.
16. Z. Ranjbar, S. Moradian, S. Rastegar, Formation of a percolating cluster in films prepared by cathodic electrodeposition of a mixture of lower and higher molecular weight epoxy–amine adducts, *J. Colloid Inter. Sci.*, 264(2003), 420-430.
17. P. Visser, et al., The chemical throwing power of lithium-based inhibitors from organic coatings on AA2024-T3, *Corr. Sci.*, 150(2019), 194-206.
18. T. Wang, et al., Preparation and surface characteristics of low-temperature curing fluorinated cathodic electrodeposition coating, *Prog. Organic Coat.*, 60(2007), 132-139.

19. A. Nasresfahani, L. A. Idowu, R. A. Hutchinson, Extractable content of functional acrylic resins produced by radical copolymerization: A comparison of experiment and stochastic simulation, *Chem. Eng. J.*, 378(2019), 122087.
20. A. Tiwari, L. Hihara, J. Rawlins, Intelligent coatings for corrosion control, 2014, Butterworth-Heinemann.
21. G. Brug, et al., The analysis of electrode impedances complicated by the presence of a constant phase element, *J. Electroanal. Chem*., 176(1984), 275-295.
22. B. Hirschorn, et al., Determination of effective capacitance and film thickness from constant-phase-element parameters, *Electrochim. Acta*, 55(2010), 6218-6227.
23. S. P. Harrington, T. M. Devine, Analysis of electrodes displaying frequency dispersion in Mott-Schottky tests, *J. Electrochem. Soc*., 155(2008), C381-C386.
24. B. Hirschorn, et al., Constant-phase-element behavior caused by resistivity distributions in films II. Applications, *J. Electrochem. Soc*., 157(2010), C458-C463.
25. G. Qiao, J. Ou, Corrosion monitoring of reinforcing steel in cement mortar by EIS and ENA, *Electrochim. Acta*, 52(2007), 8008-8019.
26. Z. Ranjbar, S. Moradian, Characteristics and deposition behavior of epoxy–amine adducts in cathodic electrodeposition as a function of the degree of neutralization, *Coll. Surf. A*. 219(2003), 147-59.
27. Y. I. Suzuki, H. Fukui, K. Tsuchiya, S. Arita, Y.H.Ogata, Correlation of film structure with film formation in cationic electropaint systems: An ionically conductive model, *J. Electrochem. Soc.*, 150(2003), C115.
28. N. Furuno, H. Kawai, Y. Oyabu, Mechanism of film formation by the electrodeposition coating, *J. Colloid Inter. Sci*., 55(1976), 297-304.

How to cite this article:
M. Haghi, Z. Ranjbar, H. Kazemian, M. Aghili, Synthesis, Characterization and Corrosion Resistance Behavior of Waterborne Cationic Acrylic Resins. Prog. Color Colorants Coat., 16 (2023), 31-45.